Blue Widefield Images of Scanning Laser Ophthalmoscope Can Detect Retinal Ischemic Areas in Eyes With Diabetic Retinopathy

Shintaro Horie
Tokyo Medical and Dental University
Nobuyuki Kukimoto
Tokyo Medical and Dental University
Koju Kamoi
Tokyo Medical and Dental University
Tae Igarashi-Yokoi
Tokyo Medical and Dental University
Takeshi Yoshida
Tokyo Medical and Dental University
Kyoko Ohno-Matsui (k.ohno.oph@tmd.ac.jp)
Tokyo Medical and Dental University

Research Article

Keywords: Diabetic retinopathy, fluorescein angiography, retinal non-perfused areas, widefield multicolor scanning laser ophthalmoscope

Posted Date: December 10th, 2020

DOI: https://doi.org/10.21203/rs.3.rs-123877/v1

Abstract

Diabetic retinopathy (DR) is one of the leading causes of blindness worldwide. The retinal ischemic changes in DR need to be detected and treated appropriately to prevent further progression. At present, fluorescein angiography (FA) is the most commonly used method to detect the ischemic areas.

We present our results that showed a practical method of detecting retinal ischemic area covering mid-peripheral retina by multicolor widefield scanning laser ophthalmoscopy (SLO) without fluorescein. Ninety patients with and 50 patients without diabetes mellitus were studied retrospectively. All had undergone multicolor widefield SLO imaging.

Hyporeflective areas in blue image of SLO were found in the incidence of 76.6% in eyes with proliferative DR eyes. In a comparison of the hyporeflective areas of the blue SLO images to the non-perfused areas in the FA images, the appearance and the correspondence in the locations of these findings in the two types of images were found, and the incidence were highly concordant with Cohen kappa value of 0.785.

The high concordance between the hyporeflective areas in the wide-field blue SLO images and the NPAs in the FA images indicates that this method can be clinically useful to identify ischemic retinal areas in DR.

Introduction

Diabetic retinopathy (DR) is a leading cause of blindness worldwide [1–3], and a further increase in the number of diabetic patients is anticipated in the future. The increase in the incidence of DR is not only in developed but also in undeveloped countries, and it is a consequence of urbanization, population aging, and changing lifestyle [4–7]. Accordingly, DR and its vision-threatening complications such as macular edema, proliferative DR (PDR) and neovascular glaucoma are emerging problems in ophthalmology throughout the world [8,9].

The lesions in eyes with DR are most likely caused by chronic retinal ischemia in the non-perfused retinal areas (NPAs). The ischemia also causes the release of vascular endothelial growth factor (VEGF) from the cells surrounding the NPAs, and the additional VEGF induces a progression of the DR to PDR [10,11]. Once NPAs are identified, they are treated by photocoagulation to prevent the development of neovascularization and the progression of nonproliferative DR (NPDR) to PDR.

Fluorescein angiography (FA) has been the gold standard technique to detect the NPAs, but the recent introduction of widefield FA has been shown to be more helpful for detecting the NPAs that are widely distributed throughout the retina [12,13]. However, FA is an invasive technique because it requires an intravenous injection of fluorescein, and it cannot be performed on all patients.

OCT angiography (OCTA) is a relatively new technique that can detect retinal blood vessels including capillaries without requiring intravenous dye injections [14–16]. The advent of widefield OCTA has allowed clinicians to examine wider areas of the fundus [17]. However, obtaining clear OCTA images of the periphery by conventional OCT devices is difficult especially in eyes with media opacities.

The advantages of widefield image compared to conventional devices are not only its ease in obtaining wide areas of the fundus but it also allows the acquisition of seamless images avoiding the absence of some areas of the far periphery. This is especially critical in finding all of the retinal ischemic areas in eyes with DR or RVO. At present, widefield imaging and multicolor SLO imaging can be performed by the Optos® and Mirante® (NIDEK, Aichi, Japan) devices. The Mirante® device is a multimodal imaging ophthalmic instrument whose image covers a field of view of 163 degrees. The color images are obtained by red, green, and blue confocal lasers. Although the field of view of this instrument is narrower than Optos® which has a 200 degree field of view, the Mirante® has an additional blue laser with the green and red lasers. Thus, the characteristics of the images obtained by SLO are different. When a widefield color image is recorded, the original single blue, green, and red SLO images are obtained simultaneously. In the multicolor SLO, the appearance of the lesion is different for each color image because the penetration of the different colors of laser is different [18,19].

Shin et al. reported that the hyporeflective areas in the red-free blue SLO images corresponded with the NPAs in eyes with DR and retinal vein occlusion (RVO) [20]. However, they used an SLO with the conventional field of view, and the smaller visual field of view was a limitation because NPAs in DR or RVO are frequently seen in the mid-periphery of the fundus. Recent availability of widefield image in blue SLO by has allowed us to examine a wider area of the retina.

Thus, the purpose of this study was to investigate the concordance of widefield blue SLO and FA findings throughout fundus and to evaluate the usefulness of new method in detecting vast NPAs of DR in this non-invasive and relatively easy method.

Methods

Study design and Patients

This study was retrospective observational case series. We examined the medical records of patients with diabetes mellitus (DM) and non-DM controls who had been examined in the outpatient clinic of the Department of Ophthalmology and Visual Science at Tokyo Medical and Dental University (TMDU). All of the subjects had undergone multicolor widefield SLO imaging with the Mirante® device (NIDEK, Aichi, Japan) between February 2020 and July 2020. The DM eyes were classified as proliferative diabetic retinopathy (PDR), moderate to severe nonproliferative diabetic retinopathy (NPDR), or less than mild NPDR according to the classification by global diabetic retinopathy project group [25]. The control patients included those with RVO and other retinal diseases that can develop NPAs. Eyes with other disorders not affecting the retina such as anterior uveitis, dry eyes, cataracts, or the unaffected fellow eyes of patients

with unilateral retinal disorders served as controls. Patients excluded were those under 20-years-of-age, and those whose SLO images were not clear due to media opacities.

The Ethics Committee of Tokyo Medical and Dental University approved the procedures used in this study, and they conformed to the tenets of the Declaration of Helsinki.

Widefield multicolor scanning laser ophthalmoscopy (SLO) and multimodal imaging

All patients underwent multicolor widefield SLO fundus photography with the Mirante® device (NIDEK, Aichi, Japan). With this device, blue (480 nm), green (532 nm), and red (670 nm) wavelength images of the fundus were recorded along with the synthesized color images (Supplementary Fig. 1). The widefield SLO images were taken with an additional attachment to the camera to increase the field of view to 163 degrees. Both the blue and synthesized color SLO images were examined. When available, fluorescein angiograms (FA) taken with a conventional fundus camera (KOWA Vx10-i®, Tokyo, Japan) or with a SLO camera (HRA Spectlalis®, Heidelberg, Germany or NIDEK Mirante® Aichi, Japan) were also evaluated. In some cases, the OCT images were obtained with an ultra wide-field OCT device (Canon Xephilio®, Kyoto, Japan).

Statistical analyses

Unpaired non parametric Man-Whitney U-tests or Kruskal-Wallis tests were used to determine the significance of the differences in the age, refractive error, and best-corrected visual acuity (BCVA) among the eyes with moderate to severe NPDR, less than mild NPDR, RVO, fundus diseases except DR and RVO, and non-retinal diseases. Chi-square tests were used to determine the significance of the differences in the sex distribution. The concordance between the hyporeflective areas in the blue widefield SLO images and the NPAs observed in the FA images was determined by calculating Cohen's kappa coefficient (κ). We considered a κ value > 0.8 as almost perfect concordance and between 0.6 and 0.8 as substantial concordance. A P-value of < 0.05 was considered statistically significant. Statistical analyses were performed using GraphPad Prism® (GraphPad Software. Inc. Ver. 6.0).

Results

Demographics of patients (Table 1)

The medical records of 177 eyes of 90 DM patients were reviewed; 5 patients had type 1 DM and 85 patients had type 2 DM. In the DM group, 94 eyes of 51 patients (53.1%) had PDR, 53 eyes of 32 patients (29.9%) had moderate/severe NPDR, and 30 eyes of 16 patients (16.9%) had less than mild NPDR. Nine patients had signs of a different stage in one eye from that of the other one. Ninety-eight of the 177 eyes (55.4%) had received panretinal retinal photocoagulation (PRP) or local photocoagulation; 63 eyes with PDR, 35 eyes with moderate/severe NPDR, and none with less than mild NPDR. Fifty-three of the 177 eyes (29.9%) had received anti-VEGF therapies, and 33 of the 94 PDR eyes (35.1%) had undergone pars plana vitrectomy.

For the non-DM controls, 99 eyes of 50 patients who had widefield SLO examinations during the same period were analyzed. The control eyes included 7 eyes of 6 patients with RVO, 47 eyes of 34 patients with other retinal disorders, and 45 eyes of 36 patients without any retinal disorders. All 7 eyes with RVO had a branch retinal vein occlusion (BRVO). Other fundus diseases included 7 eyes with an epiretinal membrane, 7 eyes with Vogt-Koyanagi-Harada disease, 4 eyes with a rhegmatogenous retinal detachment, 4 eyes with multifocal posterior pigment epitheliopathy, 3 eyes with glaucoma, 3 with a macular hole, 3 with a peripheral vasoproliferative tumor, 2 eyes with dry AMD, 2 eyes with sarcoidosis, and 2 eyes with panuveitis. There were 45 eyes without any fundus disorders including the unaffected fellow eyes of patients with unilateral fundus disorders (23 eyes), dry eye (7 eyes), anterior uveitis (5 eyes), and cataract (3 eyes). Widefield SLO images were taken as one of the routine ocular examinations in these patients without fundus disorders.

Comparisons of the demographics of the DM group and controls are shown in Table 1. The differences in the mean age (63.0 ± 12.3 years in DM and 62.9 ± 14.8 in controls) and the mean refractive error (-1.6 ± 2.6 D in DM and − 3.2 ± 4.6 D in controls) were not significant. The DM patients had significantly poorer decimal BCVA than controls (0.29 ± 0.40 vs. 0.08 ± 0.26). There were significantly more men in the DM group than in the control group.

We also compared the demographics of the PDR, moderate/severe NPDR, less than mild NPDR, RVO, other fundus diseases, and no fundus diseases groups. The results showed that there were significant differences in the sex distribution, age, and BCVA ($P < 0.001$ in Chi-square test; $P < 0.05$ and $P < 0.001$ in Kruskal-Wallis test). There was no significant difference in the refractive error among the 6 groups (Kruskal-Wallis tests; Table 1).

Presence of hyporeflective areas in blue widefield SLO images in eyes with advanced diabetic retinopathy (DR)

In patients with no fundus lesions, a uniform background was observed in the blue widefield blue images (Supplementary Fig. 1). On the other hand, hyporeflective areas were present in the blue widefield SLO images in 98 of the 177 eyes of the DM patients (55.4%; Figs. 1–5, Table 2). A hyporeflective area was easily recognized as an area of darker appearance than the surrounding areas. In some areas, the retinal vessels crossing the hyporeflective area were seen as white lines (Fig. 1–5). Hyporeflective areas were found in 72 of 94 eyes with PDR (76.6%), in 26 of the 53 eyes (49.1%) with moderate to severe NPDR, and none of the 30 eyes (0%) with less than mild NPDR. The hyporeflective areas were either localized or diffuse. Among the 72 eyes with PDR that had hyporeflective areas, 63 eyes (87.5%) had a history of PRP. In these 63 eyes, hyporeflective areas were observed both in eyes with and without prior PRP (Figs. 1–5).

Among the control patients, hyporeflective areas were not found in the blue SLO images in any of the 56 eyes with any fundus diseases other than in eyes with RVO. However, hyporeflective areas in the blue SLO images were seen in 4 of 7 (57.1%) eyes with a BRVO (Table 2). None of the 36 control eyes with fundus disorders had hyporeflective areas.

Concordance of hyporeflective areas in blue widefield SLO images and non-perfused areas (NPAs) in fluorescein angiograms (FA)

FA images were available for 175 eyes; 126 eyes in the DM groups and 49 eyes in the non-DM controls. In the DM group, 70 of the 94 eyes with PDR had FA images, 46 of the 53 eyes with moderate to severe NPDR had FA images, and 10 of the 30 eyes with less than mild NPDR had FA images. Among the 49 eyes of the non-DM controls, FA images were available in 6 of the 7 eyes with BRVO, 35 of the 56 eyes with fundus disorders except DR or RVO, and 8 of the 36 eyes with non-fundus disorders.

Among the eyes examined by FA, NPAs were found in 65 eyes with PDR, in 27 eyes with moderate to severe NPDR, and in 3 eyes with BRVO. In these cases, a concordance in the incidence and location between the hyporeflective area in the blue SLO images and the NPAs in the FA images was evaluated (Table 3). Among the 65 eyes with PDR in which NPAs were found in the FA images, hyporeflective areas in the blue SLO images were observed in 53 eyes (52/65, 80.0% sensitivity). Similarly, in 27 eyes with moderate to severe NPDR and with NPAs in the FA images, the hyporeflective areas in the blue SLO images were found in 21 eyes (21/27, 77.8% sensitivity). In these eyes, the location of the hyporeflective areas corresponded exactly within the location of the NPAs in the FA images (Fig. 1–5). In contrast, 13 of the 65 eyes (19.7%) with PDR and with NPAs in the FA images and 6 of the 27 eyes (22.2%) with moderate to severe NPDR and with NPAs did not show hyporeflective areas in the blue SLO images. In these eyes, the SLO images were obtained after photocoagulation, while the FA images were obtained before the treatment. Thus, the chorioretinal scars of photocoagulations seemed to interfere with finding the dark areas with multiple scars showing hyperreflection. In 3 eyes with BRVO and with NPAs in the FA images, the hyporeflective areas were detected in all 3 eyes (3/3, 100% sensitivity). In these 3 eyes, the hyporeflective areas corresponded with the areas of the NPAs in the FA images (Supplementary Fig. 2).

In contrast, none of the eyes without a NPA in the FA images (10 eyes with less than mild NPDR, 3 eyes with BRVO, 35 eyes with other fundus diseases except DR/RVO, and 8 eyes without fundus diseases) showed any hyporeflective areas in the blue widefield SLO images.

The concordance between the incidence of hyporeflective areas in the widefield blue SLO and the NPAs in the FA images was determined by calculating Cohen's kappa coefficient (κ) with the kappa function. The mean κ value was 0.785 with a range of 0.6 and 0.8. Thus, we conclude that there was good concordance in the incidence (Table 3). Furthermore, hyporeflective areas were not found in the blue SLO images, when NPAs in the FA images were not found, in all 80 eyes for a specificity of 100%. Thus, the concordance relationship between the widefield blue SLO images and the NPAs in the FA images was very high.

Thinning and disorganization of retina in hyporeflective areas in blue widefield SLO images

Ultra-widefield OCT findings were examined to determine the morphological changes of the retina in the hyporeflective areas in the blue SLO images. There were images from both widefield SLO images and corresponding OCT images of 3 eyes in 2 cases. In these 3 eyes, the area of dark findings in the blue SLO images corresponded to the NPAs detected in the FA images. In the ultra-widefield OCT images, a thinning of the entire retina with partially disorganization of the inner retinal layer was observed corresponding to the hyporeflective areas in the SLO blue images (Figs. 4,5 and supplementary Fig. 3).

Discussion

The blue widefield images showed hyporeflective areas in a high percentage of patients with PDR. Among the 92 eyes with NPAs in the FA images due to PDR or moderate/severe NPDR, 52 eyes with PDR and 21 eyes with moderate/severe NPDR had hyporeflective areas in the blue SLO images (79.3%). A high concordance of the incidence of hyporeflective areas in the blue SLO and the NPAs in the FA images was confirmed with a kappa = 0.785. In addition, a direct comparison between the FA and blue SLO images showed that the location of the hyporeflective areas seen in the blue SLO images were also found within the location of the NPAs identified in the FA images in patients with PDR and moderate to severe NPDR.

The concordance between hyporeflective areas found in blue SLO image and NPAs in FA was comparable to the findings of Shin et al [20]. However, our findings were made in almost entire continuous fundus images while the previous study examined a relatively segmented narrower field. Our findings should be especially helpful in the management of DR because the ischemia of retina in DR is not limited to only the posterior pole but throughout fundus including the periphery. Additionally, we examined the retinal structure in the ultra-widefield OCT images corresponding to the hyporeflective areas in blue SLO, and we found morphological change including a thinning and disorganization of the retina indicating secondary ischemic degeneration of the retina.

The widefield images obtained by multicolor SLO (Mirante®) cover up to the equator (163 degree field of view), which give us comprehensive information of retinal ischemia of DR in a single image. Compared to the widefield OCTA images, the blue SLO images can be easily obtained with a single shot as in the conventional fundus photographs. Blue, green, and red images are instantly recorded separately. Thus, once multicolor images are obtained, the detection of hyporeflective areas in the blue images is possible. This correspondence was also found in eyes with BRVO although the number of eyes was small. These findings suggest that the hyporeflective areas in the blue widefield SLO images are good indicators of the presence of NPAs regardless of the disease.

Despite the high concordance between the number and locations of the hyporeflective areas and the NPAs, approximately 20% of DR eyes with NPAs did not have hyporeflective areas in the blue SLO images. One of the reasons for this was that the SLO images were not taken on or around the same day as the FA examinations in some eyes. In most cases, the SLO images were taken after the targeted photocoagulation of the NPAs or after PRP, while the FA images were taken before the photocoagulation. The chorioretinal scars of photocoagulation are occasionally seen as hyperreflective areas in the blue SLO images, and this brightness often makes it difficult to detect the hyporeflective areas in the blue SLO images especially in the areas with a large number of photocoagulation scars. In some cases, media opacities such as mild vitreous hemorrhages of onset after the FA examination also reduced the resolution of the SLO images.

Recent advances in OCT technology has allowed recordings that can reveal a disorganization of the inner retinal layer in the areas where the NPAs are located in eyes with DR [21,22]. In addition, a thinning of the inner retina in the areas of the NPAs has been reported [22]. Despite the limited number of cases examined, ultra-widefield OCT was able to show the thinning and disorganization of the inner retina in the areas where the NPAs were located. Thus, it is highly likely that the hyporeflective areas in the blue SLO images represent morphological changes of the retina caused by non-perfusion in the retinal capillaries.

This study has several limitations. The study was conducted at a single tertiary eye center thus the results may not be applied to the general DR population. A second limitation is that the SLO and FA images were not always taken on the same day. Thus, an interval between the two examinations may have affected the findings.

In conclusion, these results indicate that widefield blue SLO can be used as a non-invasive and easy method to detect NPAs, and thus determine the severity of the DR. As automated screening for DR has been and will be more widely used [23,24], this technique of detecting NPAs by just one fundus photograph is considered an important and easy technique for the clinical management and screening for DR. We also conclude that these findings will not only allow clinicians to detect NPAs accurately and easily, but will also allow a monitoring of the effectiveness of therapy in slowing or halting the progress of DR.

Declarations

Acknowledgements

We thanks to Professor Emeritus Duco Hamasaki of the Bascom Palmer Eye Institute for discussions and corrections of this manuscript.

Author Contributions

Figure and manuscript preparation: SH, KOM, Concept/Rationale: SH, KOM, Study design: SH, KOM, Data collection: SH, NK, Data analysis: SH, NK, Interpretation: SH, NK, KOM, Critical review on manuscript: All authors

Competing interest

S.H. and T.Y. belong to department of Advanced Ophthalmic Imaging in Tokyo Medical and Dental University, which is funded by NIDEK Corporation. There is no other conflict of interest. The other authors: NK., KK, TIY. KOM. have no competing interest related to this submission.

Data availability

The data in this study are subject to restrictions and are not being made publicly available. Data are available only on reasonable request and with permission of ethics committee of our institution.

References

1. Yau, J. W. Y. *et al.* Global prevalence and major risk factors of diabetic retinopathy. *Diabetes Care* **35,** 556–564 (2012).
2. Flaxman, S. R. *et al.* Global causes of blindness and distance vision impairment 1990-2020: a systematic review and meta-analysis. *Lancet Glob Health* **5,** e1221–e1234 (2017).
3. Zhang, X. *et al.* Prevalence of diabetic retinopathy in the United States, 2005-2008. *JAMA* **304,** 649–656 (2010).
4. Sabanayagam, C., Yip, W., Ting, D. S. W., Tan, G. & Wong, T. Y. Ten Emerging Trends in the Epidemiology of Diabetic Retinopathy. *Ophthalmic Epidemiol* **23,** 209–222 (2016).
5. Wang, L. Z. *et al.* Availability and variability in guidelines on diabetic retinopathy screening in Asian countries. *Br J Ophthalmol* **101,** 1352–1360 (2017).
6. Ruta, L. M. *et al.* Prevalence of diabetic retinopathy in Type 2 diabetes in developing and developed countries. *Diabet Med* **30,** 387–398 (2013).
7. Guariguata, L. *et al.* Global estimates of diabetes prevalence for 2013 and projections for 2035. *Diabetes Res Clin Pract* **103,** 137–149 (2014).
8. Kume, A. & Kashiwagi, K. Recent epidemiological status of ocular and other major complications related to diabetes mellitus in Japan. *Ophthalmologica* (2020) Epub ahead of print.
9. Miyazaki, M. *et al.* Comparison of diagnostic methods for diabetes mellitus based on prevalence of retinopathy in a Japanese population: the Hisayama Study. *Diabetologia* **47,** 1411–1415 (2004).
10. Adamiec-Mroczek, J. & Oficjalska-Młyńczak, J. Assessment of selected adhesion molecule and proinflammatory cytokine levels in the vitreous body of patients with type 2 diabetes–role of the inflammatory-immune process in the pathogenesis of proliferative diabetic retinopathy. *Graefes Arch Clin Exp Ophthalmol* **246,** 1665–1670 (2008).
11. Nawaz, I. M. *et al.* Human vitreous in proliferative diabetic retinopathy: Characterization and translational implications. *Prog Retin Eye Res* **72,** 100756 (2019).
12. Mustafı, D., Saraf, S. S., Shang, Q. & Olmos de Koo, L. C. New developments in angiography for the diagnosis and management of diabetic retinopathy. *Diabetes Res Clin Pract* **167,** 108361 (2020).
13. Nicholson, L. *et al.* Retinal Nonperfusion Characteristics on Ultra-Widefield Angiography in Eyes With Severe Nonproliferative Diabetic Retinopathy and Proliferative Diabetic Retinopathy. *JAMA Ophthalmol* **137,** 626–631 (2019).
14. Tey, K. Y. *et al.* Optical coherence tomography angiography in diabetic retinopathy: a review of current applications. *Eye Vis (Lond)* **6,** 37 (2019).

15. Ashraf, M. *et al.* Vascular Density of Deep, Intermediate and Superficial Vascular Plexuses Are Differentially Affected by Diabetic Retinopathy Severity. *Invest. Ophthalmol. Vis. Sci.* **61,** 53 (2020).
16. Samara, W. A. *et al.* Quantification of Diabetic Macular Ischemia Using Optical Coherence Tomography Angiography and Its Relationship with Visual Acuity. *Ophthalmology* **124,** 235–244 (2017).
17. Sawada, O. *et al.* Comparison between wide-angle OCT angiography and ultra-wide field fluorescein angiography for detecting non-perfusion areas and retinal neovascularization in eyes with diabetic retinopathy. *Graefes Arch Clin Exp Ophthalmol* **256,** 1275–1280 (2018).
18. Terasaki, H. *et al.* Ability of MultiColor scanning laser ophthalmoscope to detect non-glaucomatous retinal nerve fiber layer defects in eyes with retinal diseases. *BMC Ophthalmol* **18,** 324 (2018).
19. Terasaki, H. *et al.* More effective screening for epiretinal membranes with multicolor scanning laser ophthalmoscope than with color fundus photographs. *Retina (Philadelphia, Pa.)* **40,** 1412–1418 (2020).
20. Shin, Y. U., Lee, B. R., Kim, S. & Lee, W. J. A novel noninvasive detection method for retinal nonperfusion using confocal red-free imaging. *Ophthalmology* **119,** 1447–1454 (2012).
21. Nicholson, L. *et al.* Diagnostic accuracy of disorganization of the retinal inner layers in detecting macular capillary non-perfusion in diabetic retinopathy. *Clin Exp Ophthalmol* **43,** 735–741 (2015).
22. Moein, H.-R. *et al.* Optical coherence tomography angiography to detect macular capillary ischemia in patients with inner retinal changes after resolved diabetic macular edema. *Retina (Philadelphia, Pa.)* **38,** 2277–2284 (2018).
23. Rajalakshmi, R., Subashini, R., Anjana, R. M. & Mohan, V. Automated diabetic retinopathy detection in smartphone-based fundus photography using artificial intelligence. *Eye (Lond)* **32,** 1138–1144 (2018).
24. Rajalakshmi, R. *et al.* Validation of Smartphone Based Retinal Photography for DiabeticRetinopathy Screening. *PLoS One* **10,** e0138285 (2015).
25. Wilkinson, C. P. *et al.* Proposed international clinical diabetic retinopathy and diabetic macular edema disease severity scales. *Ophthalmology*, **110,** 1677–1682 (2003).

Tables

Table 1. Basic characteristics of the diabetic patients and non-diabetic controls

	DM total	PDR	Moderate to severe NPDR	Less than mild NPDR	Control total	BRVO	Other Fundus diseases	Without fundus diseases	P value (DM vs control)	P value (all groups)
Number of eyes (patients)	177 (90)	94 (51)	53 (32)	30 (16)	99 (50)	7 (6)	47 (34)	45 (36)		
Gender (men/women)	58/32	34/17	23/9	9/7	18/32	2/4	12/22	13/23	*p<0.01	*p<0.001
Age (mean±years,range)	63.0±12.3 (35-85)	59.5±11.6 (35-79)	67.3±10.8 (47-84)	67.3±13.6 (38-85)	62.9±14.8 (27-84)	67.8±10.6 (48-76)	60.1±15.6 (27-84)	66.1±12.5 (27-83)	†N.S.	‡p<0.05
Spherical equivalent (D, mean±SD)	-1.6±2.6	-1.7±2.3	-1.1±3.0	-2.0±3.1	-3.2±4.6	-0.4±1.3	-4.0±5.5	-2.9±4.4	†N.S.	‡N.S.
BCVA (logMAR, mean±SD)	0.29±0.40	0.32±0.43	0.29±0.33	0.02±0.17	0.08±0.26	0.09±0.17	0.15±0.32	0.01±0.18	†p<0.001	‡p<0.001

DM= diabetes mellitus; D= diopter; BCVA= best-corrected visual aquity; logMAR= logarithm of the minimum angle of resolution; PDR= proliferative diabetic retinopathy; NPDR= non proliferative diabetic retinopathy; BRVO=branch retinal vein occlusion; *Chi-square test; †Mann-Whiteney U test; ‡Kruskal-Wallis test

Table 2. Frequency of hyporeflecitve area in wide field blue SLO		
	Disease entity	Numbers of eyes with hyporeflective area in SLO/total numbers of SLO-examined eyes (%)
DM patients		
	PDR	72/94 (76.6%)
	Moderate to severe NPDR	26/53 (49.1%)
	Less than mild NPDR	0/30 (0%)
	DM total	98/177 (55.4%)
Control patients		
	BRVO	4/7 (57.1%)
	Fundus disesases except DR/RVO	0/56 (0%)
	Non-fundus diseases	0/36 (0%)
	control total	4/99 (4.0%)
DM= diabetes mellitus; PDR=proliferative diabetic retinopathy; NPDR=non proliferative diabetic retinopathy; BRVO=branch retinal vein occulusion		

Table 3. Concordance between the incidence of hyporeflective area in blue SLO and NPAs in FA		
Disease entity	SLO-Hypo(+)eyes/FA-NPA(+) eyes (%)	SLO-Hypo(-)eyes/FA-NPA(-) eyes
PDR	52/65 (80.0%)	5/5
Moderate to severe NPDR	21/27 (77.8%)	19/19
Less than mild NPDR	0/0	10/10
BRVO	3/3 (100%)	3/3
Fundus disesases except DR/RVO	0/0	35/35
Non-fundus diseases	0/0	8/8
Total	76/95 (80.0%)	80/80 (100%)
Number of observed agreements: 156 (89.14% of the observations). Number of agreements expected by chance: 86.5 (49.44% of the observations). Kappa=0.785. 95% confidence interval:0.696-0.874. The strength of agreement is substantial.		

Figures

Figure 1

Concordance of hyporeflective areas in blue widefield scanning laser ophthalmoscope (SLO) images and non-perfused areas (NPAs) in fluorescein angiographic (FA) images in eye with nonproliferative diabetic retinopathy (DR) A: Multicolor widefiled SLO image of the right fundus of a 64-year-old man with moderate NPDR showing scattered spots of retinal photocoagulation. B: Blue SLO image shows hyporeflective areas in the mid-periphery especially in the nasal and superior quadrants of the fundus. C. Widefield FA shows NPAs in the mid-periphery especially in the nasal and superior quadrants of the fundus. NPAs are also seen in the temporal periphery. D: Magnified image of image B clearly shows hyporeflective areas in the nasal to superior quadrants. E: Magnified FA image of the same area of image C shows that the locations of the NPAs correspond to the hyporeflective areas in image D.

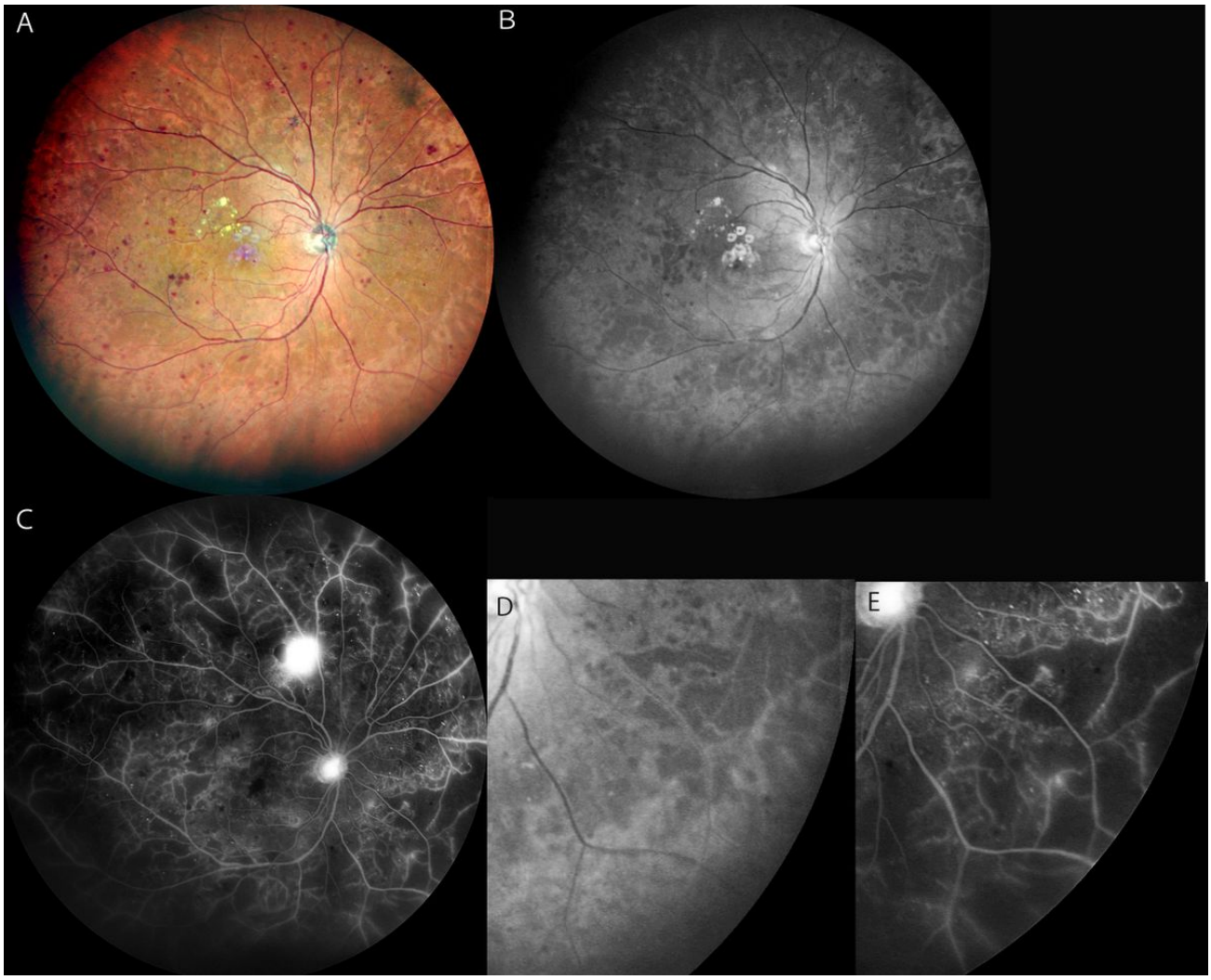

Figure 2

Concordance of hyporeflective areas in the blue widefield SLO image and NPAs in FA image in proliferative DR (PDR) with extensive NPAs and neovascularization. A: Multicolor widefield SLO image of the right fundus of a 65-year-old man with PDR showing multiple hemorrhages in a wide area of the fundus. B: Blue SLO image shows a hyporeflective area in the mid-periphery to periphery of the fundus. C: Widefield FA image shows widespread NPAs in the mid-periphery to periphery. Neovascularization is also seen in the superior pole of the eye. D: Magnified image of the B shows hyporeflective areas in the lower temporal quadrant. E: Magnified FA image of the same area as image C shows that the NPAs correspond to the hyporeflective areas in image D. Brightness and contrast have been slightly modified.

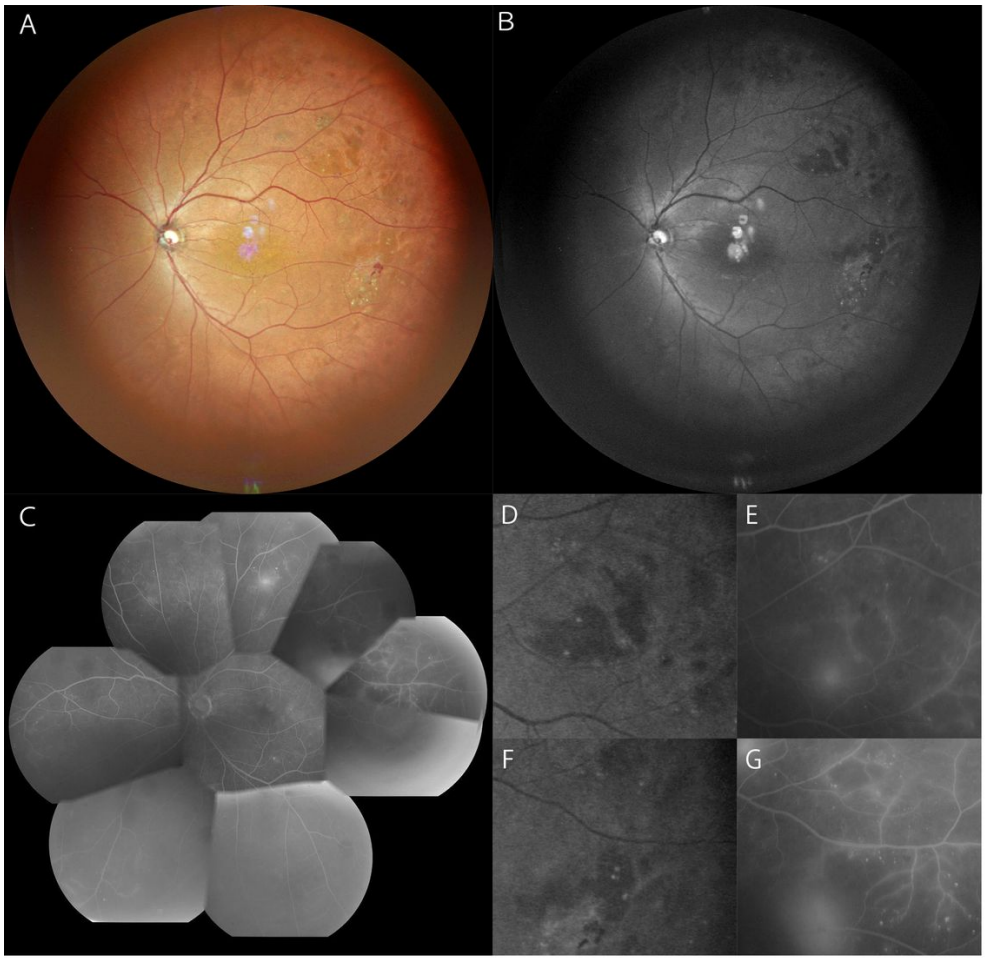

Figure 3

Concordance of hyporeflective area in blue SLO image and NPAs in FA image in PDR with focal NPAs and early neovascularization. A: Multicolor widefield SLO image of the right fundus of a 44-year-old man with PDR shows retinal hemorrhages in the temporal retina. Some dark areas are observed in the upper retina. B: Blue SLO image shows hyporeflective areas in the mid-periphery in the temporal to the upper fundus. The locations of the hyporeflective areas correspond to the dark areas observed in the multicolor SLO image. C: Panoramic FA shows NPAs in the temporal to superior fundus. Neovascularization is also present in the superior fundus. D: and F: Magnified images of B and a magnified image of FA of the same area (E, G) clearly shows that the area with hyporeflective areas in the blue SLO image correspond to the NPAs in the FA image.

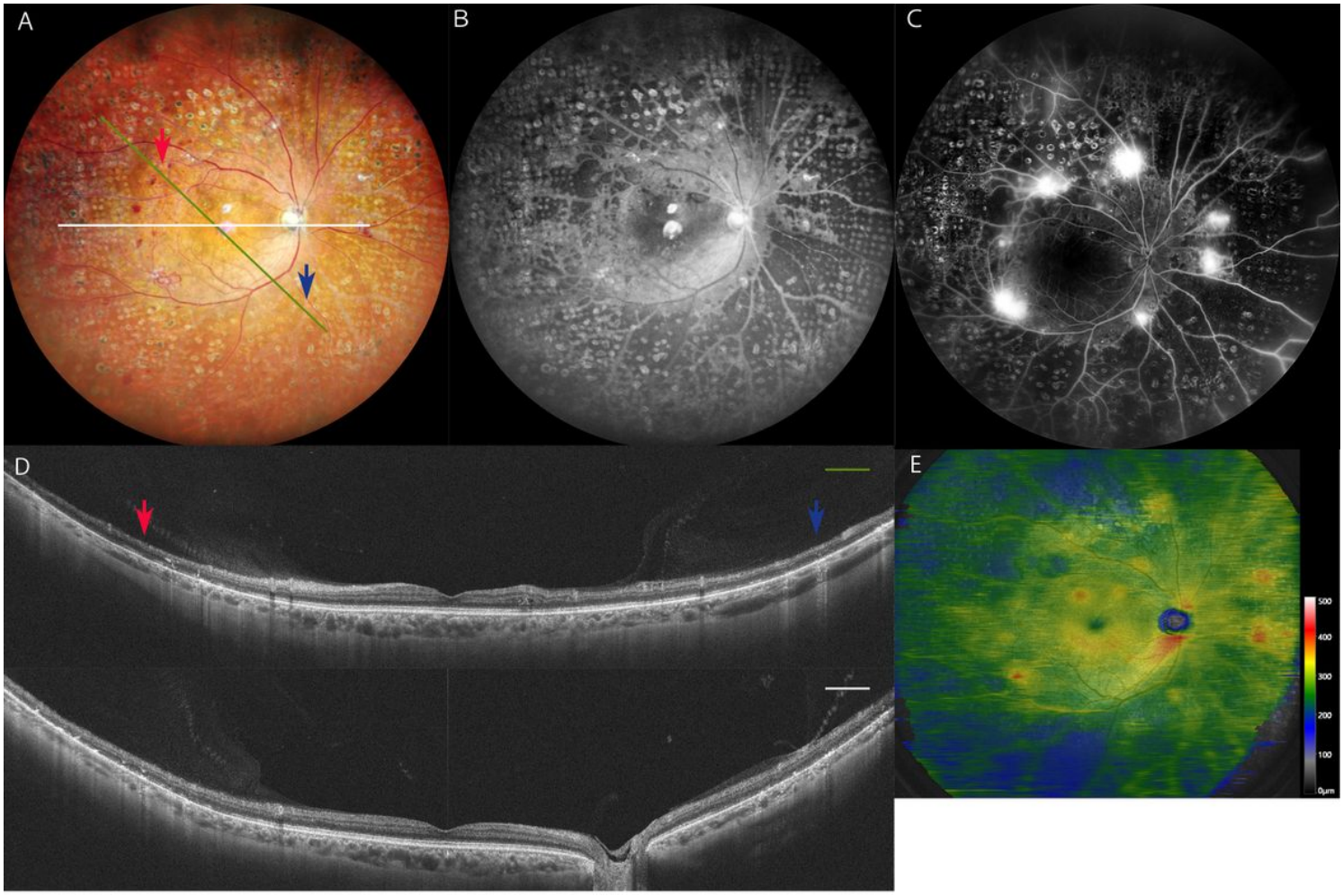

Figure 4

Comparison of hyporeflective areas in blue widefield SLO, NPAs in widefield FA and ultra wide-field OCT image in PDR with vast NPAs and multiple neovascularization. A: Multicolor widefield SLO image of the right fundus of a 55-year-old woman with PDR shows scars of panretinal photocoagulation (PRP). Red and blue arrows show corresponding points in OCT images. B: Blue SLO image shows a wide hypo-reflectance in the midperiphery and in the periphery. PRP scars show mild hyperreflectance especially in the upper fundus. C: Widefield FA shows widespread NPAs in the mid-periphery and in the periphery. Many neovascularization sites are seen along the borders of the NPAs and perfused retina. D: Oblique section of an ultra-widefield OCT image (upper image) and in a horizontal section (lower image) across the fovea show the thinning and the disorganization of inner retina (arrows) in the hyporeflective areas of the SLO image and FA image. E: Retinal thickness map of ultra-widefield OCT shows retinal thinning in the area of hypo-reflectance in the SLO image and the NPAs in the FA image.

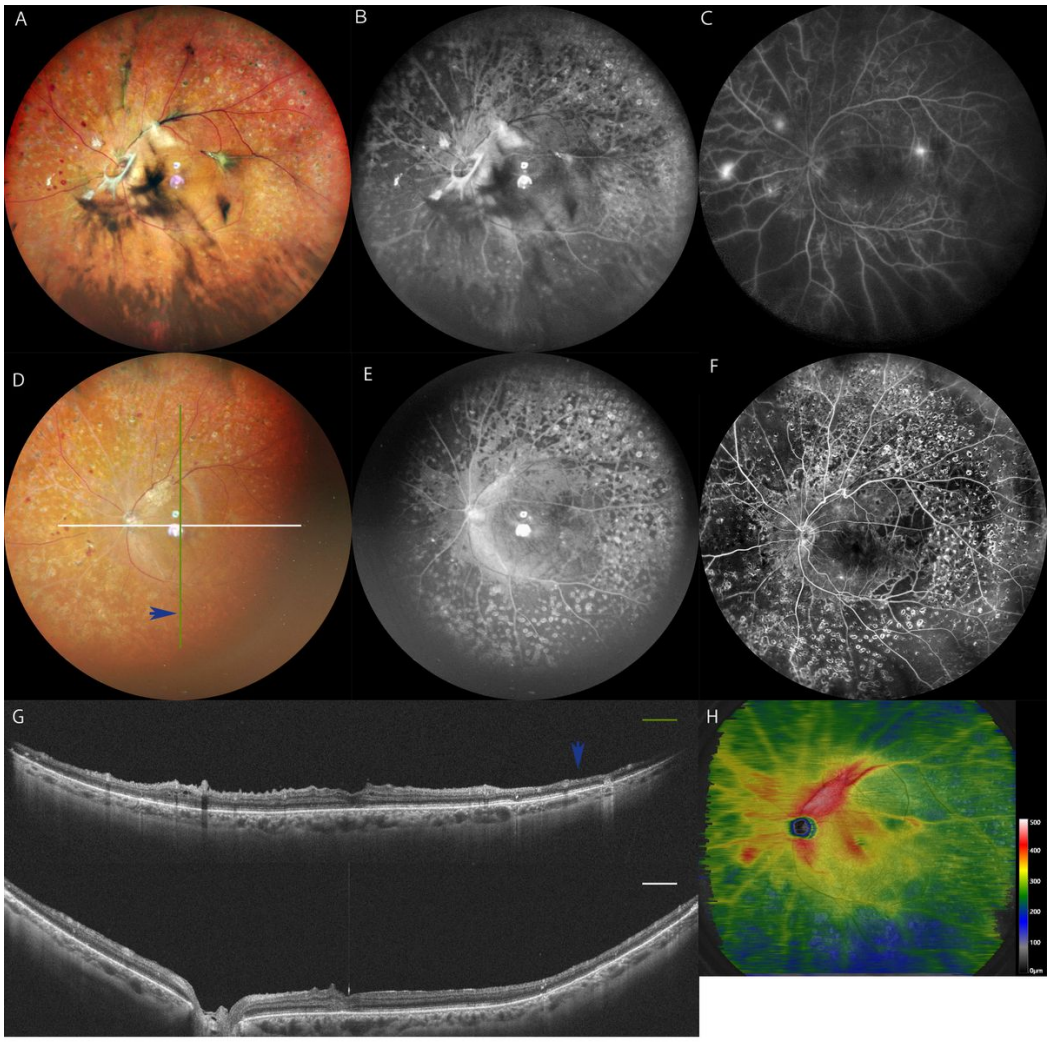

Figure 5

Thinning of the inner retina in the area of hyporeflectance in blue widefield SLO image in eye with fibrovascular proliferation of PDR A: Multicolor widefield SLO image of the right fundus of a 55-year-old woman with PDR shows vitreous hemorrhage and fibrovascular membrane especially in the peripapillary region. Arrow points to corresponding location in the OCT image. B: Blue SLO image shows a widely distributed areas of hypo-reflectance in mid-periphery and in the periphery. C: Widefield FA without prior photocoagulation (A, B) shows a wide area of NPAs D: Multicolor SLO image after pars plana vitrectomy. E: Blue SLO image after vitrectomy shows a widely distributed areas of hypo-reflectance in the mid-periphery and in the periphery. F: Widefield FA image after vitrectomy shows a wide area of NPAs at the corresponding area of hypo-reflectance in the blue SLO image (D). G: Ultra-widefield OCT images in a vertical scan (upper image) and in a horizontal scan (lower image) across the fovea show a thinning and the disorganization of the inner retina (arrows) in the hyporeflective area of the blue SLO image. H: Retinal thickness map of ultra-widefield OCT shows retinal thinning at the site of hypo-reflectance in the SLO image and the NPAs in the FA image. Brightness and contrast have been slightly modified.

Supplementary Files

This is a list of supplementary files associated with this preprint. Click to download.

- Supplementaryfigure.pdf